

Inclusion and validation of electronic stopping in the open source LAMMPS code

H. Hemani¹, A. Majalee¹, U. Bhardwaj¹, A. Arya^{2,3}, K. Nordlund⁴, M. Warrior^{1,3}

¹ Computational Analysis Division, BARC, Visakhapatnam, Andhra Pradesh 531011, India

² Glass & Advanced Materials Division, BARC, Trombay, Mumbai 400085, India

³ Homi Bhabha National Institute, Anushaktinagar, Mumbai - 400094, India

⁴ Accelerator Laboratory, Pietari Kalmin katu 2 P.O.Box 43 Helsinki, Finland

E-mail: harsh@barc.gov.in

Abstract. Electronic stopping (ES) of energetic atoms is not taken care of by the interatomic potentials used in molecular dynamics (MD) simulations when simulating collision cascades. The Lindhard-Scharff (LS) formula for electronic stopping is therefore included as a drag term for energetic atoms in the open source large scale atomic molecular massively parallel simulator (LAMMPS) code. In order to validate the ES implementatin, MD simulations of collision cascades at primary knock-on atom (PKA) energies of 5, 10 and 20 keV are carried out in W and Fe in 100 random directions. The total ES losses from the MD simulations are compared with the ES losses predicted by the Norgett-Robinson-Torrence (NRT) model. It is seen that the root mean square deviation of ES losses from the MD implementation is around 10 % for both W and Fe compared to the NRT model. The effect of ES on the number of defects in collision cascades with primary knock-on atom (PKA) energies of several tens of keV to more than 100 keV is presented.

Keywords: Electronic Stopping Collision Cascades, Molecular Dynamics, LAMMPS

1. Introduction

Energetic ions impinging on a target are slowed down by interactions with the nuclei of atoms and with the bound electrons of the target. The interactions with the nuclei depends on the repulsive potential between the atoms and is called nuclear stopping (NS). The interactions with the bound electrons of the material, and with the free electron gas if the material is a metal, is referred to as electronic stopping (ES). ES dominates NS at energies of a few tens of keV, the exact value depending on the material under consideration. The interatomic potentials used in classical MD simulations are usually obtained by fitting equilibrium properties of materials and does not include

electronic stopping. Therefore ES has to be accounted for separately in MD simulations of collision cascades.

Nuclear stopping depends on the repulsive potential between the energetic atom and the atoms of the material and is described by the semi-empirical Ziegler, Biersack and Littmark (ZBL) potential [6]. The ZBL potential is widely used to modify interatomic potentials in molecular dynamics (MD) simulations of collision cascades [7, 8]. The interatomic potentials used in MD are usually obtained by fitting equilibrium properties of materials. This does not include the inelastic collisions between a fast particle and electrons in the system i.e. electronic stopping. Therefore ES has to be accounted for separately in MD simulations of collision cascades.

The easiest way to include the effect of ES in a molecular dynamics (MD) code is by damping the velocity of an atom by a viscous force:

$$F_{es} = \beta v \quad (1)$$

where β is the drag co-efficient having units of mass/time, and, v is the velocity of the energetic atom [3]. The value of β can be obtained by several ways:

- (i) Firsov's model of mean electronic excitations in atomic collisions [9],
- (ii) Lindhard and Scharff's formula for energy dissipation of energetic ions [2],
- (iii) Finnis, et.al. formula taking into account the energy transfer from ions to a background electron gas at a specified temperature [10],
- (iv) Caro et.al's. formula including local density effects which can be implemented for interatomic potentials that use the local electron density [11], and
- (v) Nordlund, et.al., who use SRIM [6] stopping power data for the ES [12].

A different approach is taken by Duffy et.al., wherein the energy is transferred from an energetic ion to a background electron gas by frictional forces. This heats up the electron gas and subsequently raises the local temperature by thermal energy transfer between the electron gas and the ambient nuclei [13, 14]. This local hot-spot formation can have implications on the final number of defects produced and on in-cascade defect clustering. Mason et.al., have modeled the energy loss from ions to electrons using Ehrenfest dynamics [15] with a tight binding Hamiltonian wherein the electrons are not assumed to be in their ground state. They also, like Duffy et.al., treat the subsequent heat transfer from electrons to the ambient nuclei using a Langevin thermostat. They conclude that, A simple homogeneous viscous damping coefficient is adequate to model the energy transfer rate between ions and electrons, but the accuracy can be improved by making the damping constant dependent on the electron density and by computing the probabilities of specific transitions between bands [16].

LAMMPS [1] is an open source software capable of massively parallel atomistic simulations. We use it widely in our radiation damage studies, not only to simulate collision cascades [17, 18], but also to simulate defect diffusion [19, 20]. It has several package extensions amongst which the two temperature model (TTM) by Duffy et.al., is also implemented. Using the TTM, involves inputting the electron thermal conductivity

and the electron-ion interaction co-efficient which is not available for many materials of our interest. More recently, electronic stopping in LAMMPS has been introduced as a friction term with a low energy cut-off. It however needs the stopping powers to be input by the user. We calculate the stopping power within our module using the Lindhard-Scharff model to obtain a friction co-efficient and implement damping of the velocities of energetic atoms above a specified cut-off energy in LAMMPS. We validate our implementation by comparing the total energy lost by ES with the electronic loss expected from the standard NRT model [3].

This paper aims to describe the methods we have used and the validations carried out to include ES in LAMMPS. The next section describes the inclusion of ES as a friction term in MD simulations. Section.3 describes the MD runs with ES included to validate the included code for ES. Section.4 presents the results. The pros and cons of the three implementations of electronic stopping in LAMMPS mentioned in the previous paragraph is discussed at the end of section.4. Finally we present the conclusions.

2. Including Electronic Stopping in LAMMPS

ES is implemented in LAMMPS as a fix command. It is invoked as follows:

```
fix          fix-id group-id esfriction Z1 Z2 A1 A2 neval vx vy &
           vz vel-cutoff
```

where, $Z1$ and $Z2$ are the atomic numbers of the projectile and target atoms respectively and $A1$ and $A2$ are their atomic weights. The current implementation is for the case where the projectile and target atoms are the same. *neval* is the number of valence electrons of the background target element, vx,vy and vz are the X,Y,Z velocity components of the energetic PKA and *vel - cutoff* is the cutoff velocity below which there is no damping of velocities due to ES. In the following sub-sections we describe (i) the Lindhard-Scharff model for ES which we have implemented to obtain the damping factor β , and (ii) the total electron stopping losses calculation in the NRT model for validation of our implementation by obtaining the total energy loss due to ES.

2.1. The Lindhard Scharff Model for Electronic Stopping

The stopping force due to electronic drag by a target on an incoming atom having a kinetic energy E is given by

$$F_{es} = \frac{dE}{dx} = nS_{es}(E) \tag{2}$$

where, S_{es} is the electronic stopping cross section per target atom and n is the number density of the target atoms. S_{es} is given by

$$S_{es}(E) = 8\pi e^2 a_o Z_1^{1/6} \frac{Z_1 Z_2}{(Z_1^{2/3} + Z_2^{2/3})^{3/2} v_o} v = \lambda v \tag{3}$$

where v is the velocity of the energetic atom, Z_1 and Z_2 are the atomic numbers of the energetic atom and of the target respectively, a_o is the Bohr radius, e is the electronic charge, v_o is the Fermi velocity for the target atoms.

Therefore from Eqns.[1-3], we have the drag co-efficient, $\beta = n\lambda$, where λ is given by

$$\lambda = 8\pi e^2 a_o Z_1^{1/6} \frac{Z_1 Z_2}{(Z_1^{2/3} + Z_2^{2/3})^{3/2} v_o} \quad (4)$$

The Fermi velocity is the velocity is given by

$$\begin{aligned} v_o &= \sqrt{\left(\frac{2.0 * E_o}{m_e}\right)} \\ &= 5.9310e5 \sqrt{E_o} \quad (\text{in units of m/sec}) \end{aligned} \quad (5)$$

where m_e is the electron mass and E_o is the Fermi Energy given by:

$$E_o = \frac{\hbar^2}{2m_e} (3\pi^2 N_{e_{val}} * n)^{2/3} \quad (6)$$

where $N_{e_{val}}$ is the number of electrons in the outermost shell of the atom and n is the number density of the target atoms. n can easily be obtained from the lattice constant c and the number of atoms in an unit cell nat using $n = nat/c^3$.

From Eqns. [4-6], the drag co-efficient for any projectile target combination can be obtained.

2.2. Total ES loss from the NRT Model

The total loss due to ES (Q_{es}) for an energetic primary knock-on atom (PKA) in the NRT model is based on the Lindhard model. It can be obtained by finding out $E_{PKA} - \hat{E}$, where \hat{E} is the energy available to generate displacements after accounting for ES losses and is approximated by

$$\hat{E} = \frac{E_{PKA}}{[1 + kg(\epsilon)]}, \quad (7)$$

where $g(\epsilon)$ is given by

$$g(\epsilon) = 3.4008 \epsilon^{1/6} + 0.40244 \epsilon^{3/4} + \epsilon \quad (8)$$

$$k = 0.1337 Z_1^{1/6} \left(\frac{Z_1}{A_1}\right)^{1/2} \quad (9)$$

$$\epsilon = \frac{A_2 E_{PKA}}{A_1 + A_2} \frac{a}{Z_1 Z_2 e^2} \quad (10)$$

where A_1 and A_2 are the atomic numbers of the energetic atom and the target atom respectively and a is given by:

$$a = \left(\frac{9 \pi^2}{128}\right)^{1/3} a_o [Z_1^{2/3} + Z_2^{2/3}]^{-1/2} \quad (11)$$

Thus the total energy loss of the PKA due to ES, Q_{es} , is obtained from Eqns.[7-11].

2.3. Fixing a Low Energy Cut-off for Electronic Stopping

The inter-atomic potentials used in MD simulations are good enough to simulate atomic oscillations about a mean position and ES does not play a part in this dynamics. We therefore make the assumption that ES needs to be invoked only when an atom acquires sufficiently high energy to be displaced from its lattice position and settle at a new interstitial / lattice position. Therefore, the velocity corresponding to its threshold displacement energy, E_D , is a good choice for the velocity cutoff for electronic stopping, $vcut_{es}$. However, E_D depends on the direction in which an atom is launched prior to displacement by Nordlund et al., [4, 5]. They use MD simulations to obtain a direction specific threshold displacement energy which is a function of angles θ and ϕ , $E_D(\theta, \phi)$, for each lattice direction [4, 5]. An average threshold energy, E_D^{avg} , defined as the average of the function over all angles, can then be used as a Heaviside step function to decide if an atom displaces or not.

A slightly different approach is described here to obtain the threshold of displacement. MD simulations in 1000 random directions are carried out in the energy range 30-500 eV to obtain a displacement energy in Fe and W [21]. From the simulations, we obtain a direction averaged probability for displacement, which has a lower cutoff, E_D^{min} , below which there was no displacement and an upper cutoff, E_D^{max} , above which the probability of displacement is 1. For Fe, we obtained $E_D^{min} = 30eV$, $E_D^{avg} = 60eV$, $E_D^{max} = 90eV$ and for W we obtain $E_D^{min} = 30eV$, $E_D^{avg} = 150eV$, $E_D^{max} = 270eV$.

MD simulations of collision cascades with our implementation of electronic stopping with $vcut_{es}$ corresponding to E_D^{min} , E_D^{max} and their average value, say E_D^{avg} have been carried out for Fe and W. Details of the simulations are described in the next section.

3. Validating the Implementation of Electronic Stopping

MD simulations of collision cascades were carried out at 1, 5, 10 and 20 keV in W and Fe to validate the implementation of ES in LAMMPS. $52 \times 52 \times 52$ unit cells sample of W crystal was initially equilibrated using an NPT ensemble at 300 K temperature and 0 bar pressure. Similarly for Fe, $52 \times 52 \times 52$ unit cells for 1 keV and 3 keV, $72 \times 72 \times 72$ unit cells for 5 keV, $102 \times 102 \times 102$ unit cells for 10 keV and $132 \times 132 \times 132$ unit cells for 20 keV PKA were used and the crystal was equilibrated. The collision cascade simulations were then carried out by directing a centrally located primary knock-on atom (PKA) along 100 random directions at each of these energies using an NVE ensemble for 10 ps, amounting to a total of 400 MD simulations. The atoms in the outermost cells of the system were held fixed. The atoms in two unit cells lying just inside the outermost unit cell were subjected to an NVT ensemble at 300 K. Three sets of runs at each energy, for both Fe and W, were carried out corresponding to $vcut_{es}$ corresponding to E_D^{min} , E_D^{max} and E_D^{avg} as discussed in the previous section. The runs were repeated without ES to study the effect of ES on the number of defects produced. The number of defects as a function of energy for both Fe and W are calculated using the methods described in

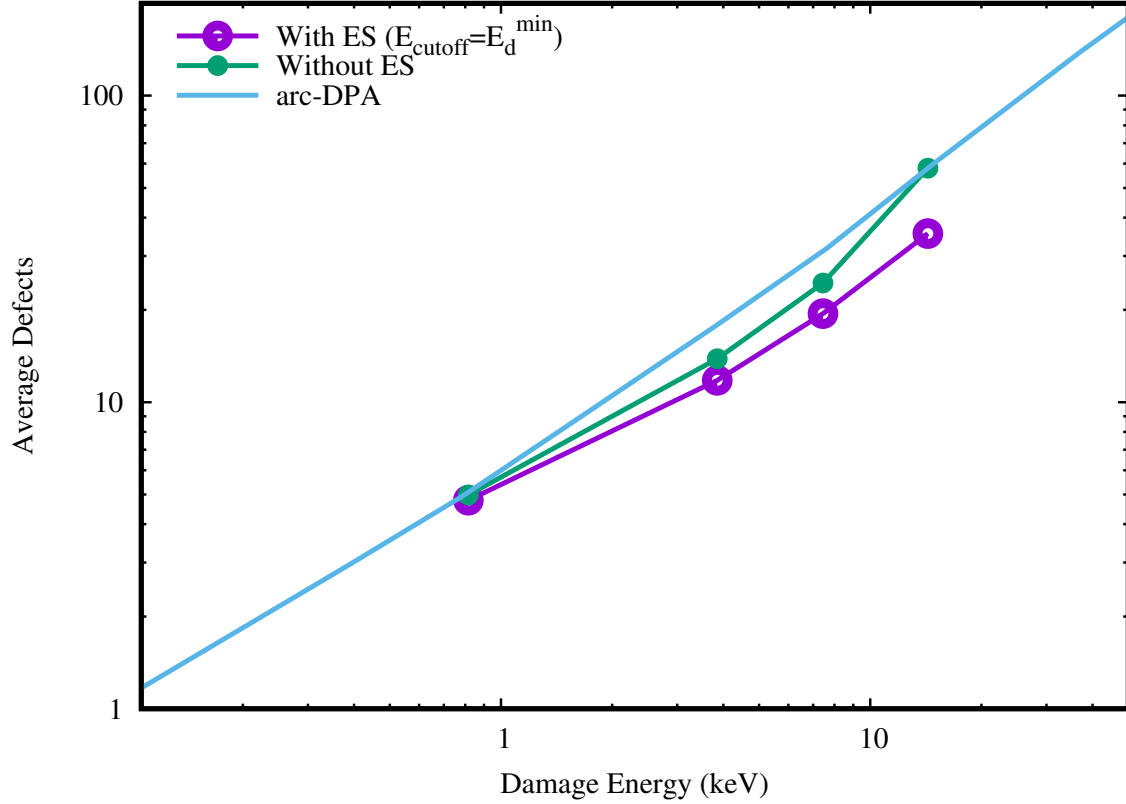


Figure 1. Number of defects in Fe as a function of damage energy in the range 1-20 keV, with and without electronic stopping. The number of defects from the arcDPA formula for Fe is also plotted for comparison

[18]. The total ES losses from the LAMMPS simulations are compared with the total ES losses obtained from the NRT model to validate the

`fix_esfriction`

code added to LAMMPS.

4. Results and Discussions

The direction averaged number of defects with and without ES for both Fe and W are shown in Fig.1 and Fig.2 respectively. The results are compared with the arcDPA formula [8]. Note that at higher PKA energies, ES losses increase and result in lower number of defects compared to the case without ES. The losses are higher at higher energies resulting in a more pronounced difference in the number of defects with and without ES.

Fig.3, Fig.4 and Fig.3 show the total electronic stopping energy loss at for the 5 keV, 10 keV and 20 keV Fe PKA in Fe using E_D^{min} , E_D^{avg} and E_D^{max} as the low energy cutoff for electronic stopping. It is seen that the choice of E_D^{min} shows the best match with the total energy loss calculated by the NRT model. A large spread in the total

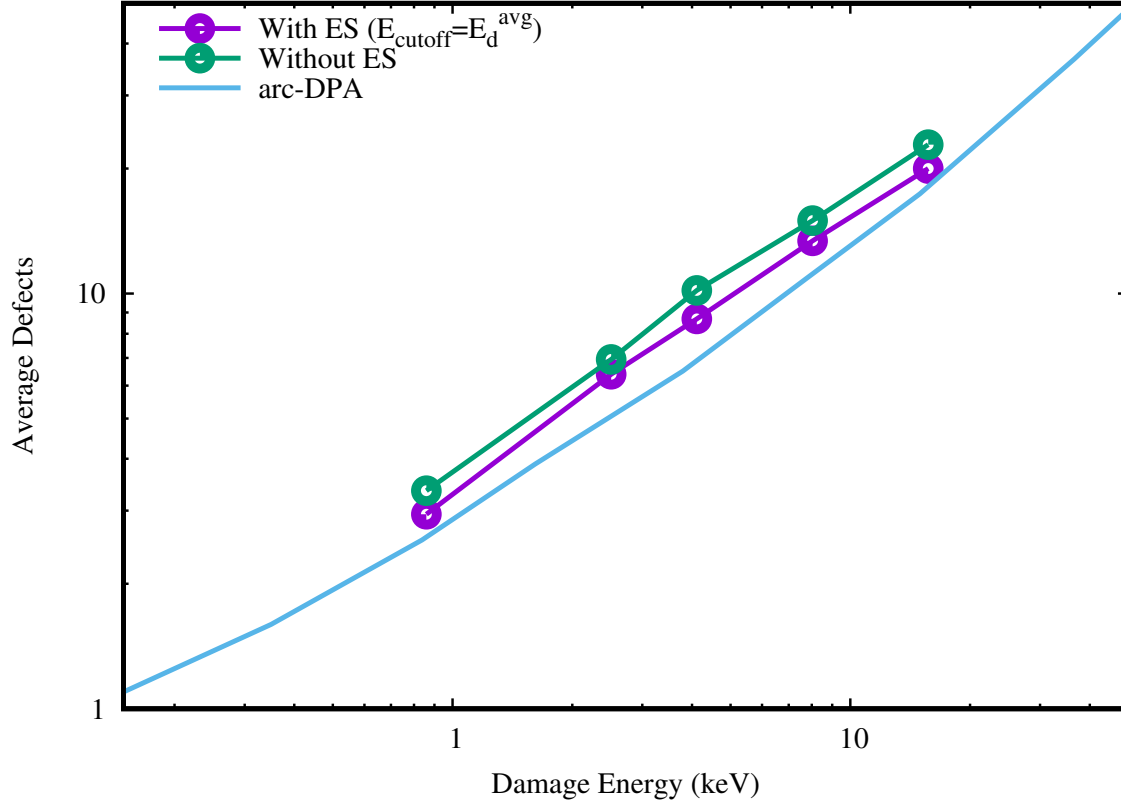


Figure 2. Number of defects in W as a function of damage energy in the range 1-20 keV, with and without electronic stopping. The number of defects from the arcDPA formula for W is also plotted for comparison

energy loss for PKAs directed in random directions is also seen in all the simulations. This variation in the total ES energy loss, is due to variations in the collision cascade trajectories for PKAs launched along the 100 random directions and is a similar effect as the straggling seen in the range of energetic atoms in materials. The large spread also has implications on the number of defects created because the energy available for damage creation will also subsequently have a large spread.

Similarly, Fig.6, Fig.7 and Fig.8 show the total electronic stopping energy loss at for the 5 keV, 10 keV and 20 keV Fe PKA in W using E_D^{min} , E_D^{avg} and E_D^{max} as the low energy cutoff for electronic stopping. The straggling in the total energy loss is seen in W too. Regarding the choice of low energy cut-off for ES, it is seen that the choice of E_D^{avg} shows the best match with the NRT model. This implies that there is no unique way to determine the best value of the low energy cutoff for ES, but a value close to E_D is a good initial choice.

A discussion on the three methods of including electronic stopping in collision cascade simulations with LAMMPS might be useful for the reader. A detailed analysis of the three methods is out of the scope of this document. We mention our viewpoint on this as follows:

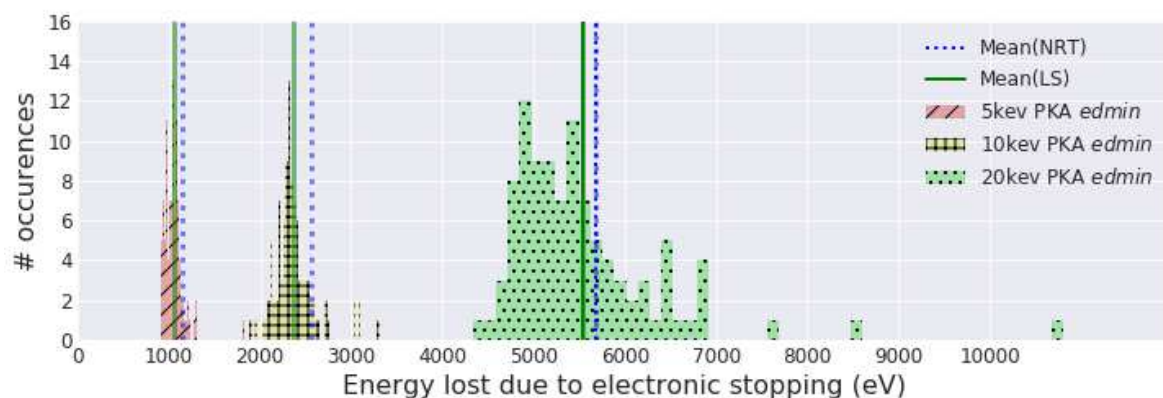


Figure 3. Electronic stopping energy loss at for the 5 keV, 10 keV and 20 keV Fe PKA in Fe using E_D^{min} as the low energy cutoff for ES. The dashed line is the total energy loss calculated from the NRT model and the solid line is the direction averaged total loss from the 100 MD simulations at each of the PKA energies.

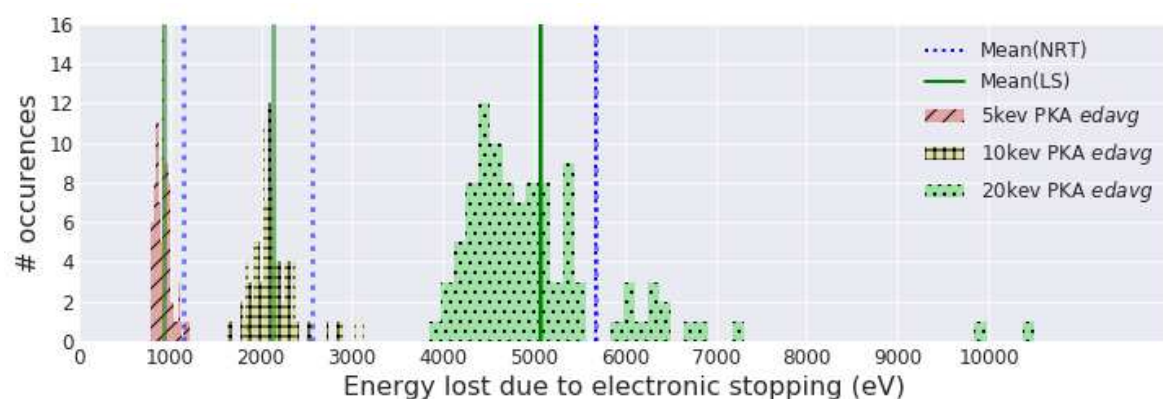


Figure 4. Electronic stopping energy loss at for the 5 keV, 10 keV and 20 keV Fe PKA in Fe using E_D^{avg} as the low energy cutoff for ES. The dashed line is the total energy loss calculated from the NRT model and the solid line is the direction averaged total loss from the 100 MD simulations at each of the PKA energies.

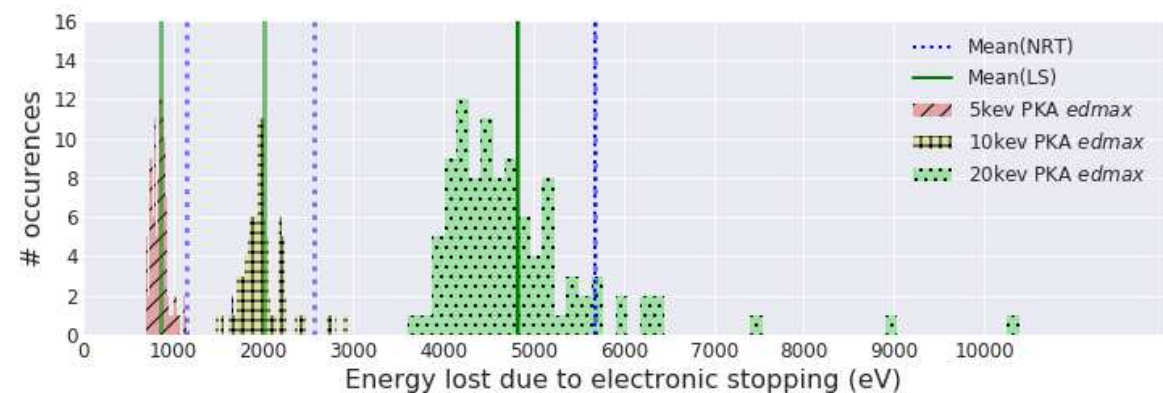


Figure 5. Electronic stopping energy loss at for the 5 keV, 10 keV and 20 keV Fe PKA in Fe using E_D^{max} as the low energy cutoff for ES. The dashed line is the total energy loss calculated from the NRT model and the solid line is the direction averaged total loss from the 100 MD simulations at each of the PKA energies.

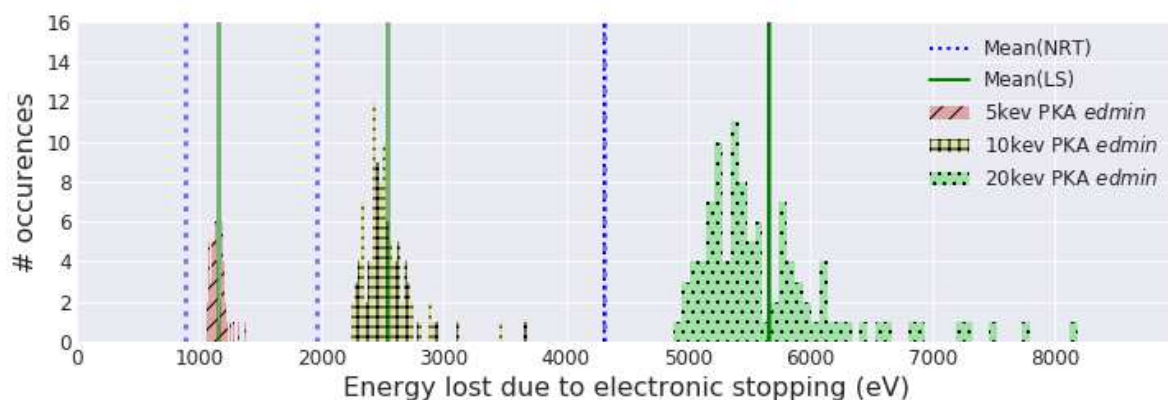


Figure 6. Electronic stopping energy loss at for the 5 keV, 10 keV and 20 keV W PKA in W using E_D^{min} as the low energy cutoff for ES. The dashed line is the total energy loss calculated from the NRT model and the solid line is the direction averaged total loss from the 100 MD simulations at each of the PKA energies.

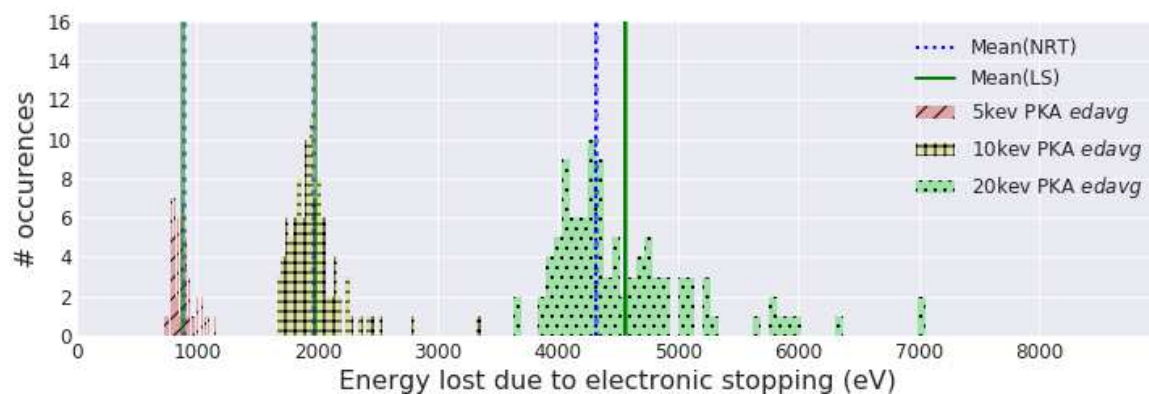


Figure 7. Electronic stopping energy loss at for the 5 keV, 10 keV and 20 keV W PKA in W using E_D^{avg} as the low energy cutoff for ES. The dashed line is the total energy loss calculated from the NRT model and the solid line is the direction averaged total loss from the 100 MD simulations at each of the PKA energies.

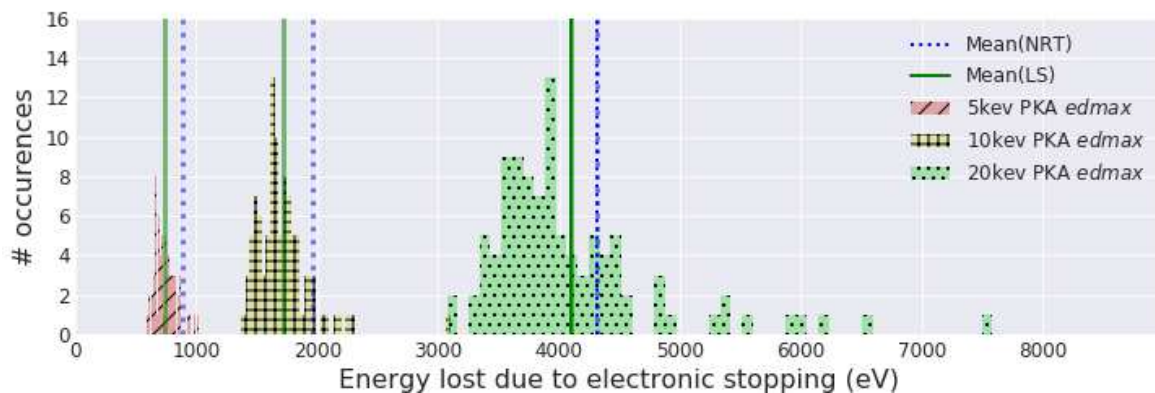


Figure 8. Electronic stopping energy loss at for the 5 keV, 10 keV and 20 keV W PKA in W using E_D^{max} as the low energy cutoff for ES. The dashed line is the total energy loss calculated from the NRT model and the solid line is the direction averaged total loss from the 100 MD simulations at each of the PKA energies.

- (i) The two temperature model [13, 14] takes care of the local temperature increase of electrons within the collision cascade and this may have implications on the in-cascade defect clustering and on defect recombination during the collision cascade.

The user has to input the following parameters:

- electronic specific heat
- electronic density
- electronic thermal conductivity
- friction coefficient due to electron-ion interactions
- friction coefficient due to electronic stopping
- electronic stopping critical velocity

An electronic sub-system is created within a specified grid in the simulation domain and the local heating of electrons, the heat transfer between electrons and ions and the subsequent heat diffusion are all taken into account using the above inputs. Therefore this is the most comprehensive model taking into account the maximum physical interactions amongst the three methods and is as accurate as the models used to input these parameters. Some of these parameters may not be known for materials of interest. We are not clear how this model treats target materials which have multiple elements (alloys). A more detailed study is necessary to understand at what primary knock on atom energies the difference in defect clustering due to using the TTM becomes important.

- (ii) The other two methods are same in the sense that both include electronic stopping as a frictional force. The only difference is that in the existing method, the user has to input the stopping power as tables and in our method it is calculated within the code. This difference has the following implications:

- The stopping power tables may be more accurate. However other codes have to be run in order to create the tables if not available to the user.
- Using stopping power tables allows calculation of electronic stopping in the case of alloys. The method developed in this work assumes a single element target.

A detailed study of the three methods and their effects on number of defects and on defect clustering needs to be carried out. This is out of scope of this paper which aims to describe our implementation of electronic stopping in LAMMPS.

5. Conclusions

Electronic stopping losses, which decreases the available energy to create defects in collision cascades, has been included in the open source Large-scale Atomic Molecular Massively Parallel Simulator (LAMMPS). This is done by implementing a new "fix" in LAMMPS called

`fix_esfriction`

which adds a friction force to all atoms moving with a velocity greater than a specified cut-off velocity. The co-efficient of the frictional force is obtained from the Lindhard-Scharf model. The code is validated by comparing the total ES loss from LAMMPS simulations with the total ES from NRT model. It is shown that ES affects the number of defects created, and at high energies of PKA, the effect of ES on the number of defects formed is more pronounced as expected. The total electronic stopping losses along different directions also show a large deviation due to straggling along the random directions of launch of the PKA and as expected, larger the PKA energy, more is the straggling. An initial choice of the low energy cut-off for ES can be the displacement energy of the atom and finer adjustments to the chosen value can be made by adjusting it so that the average total energy loss due to ES matches with that calculated by the NRT model.

References

- [1] Steve, Fast parallel algorithms for short-range molecular dynamics, *Journal of Computational Physics* 117 (1) (1995) 1 – 19. doi:<http://dx.doi.org/10.1006/jcph.1995.1039>.
- [2] J. Lindhard, M. Scharff, Energy dissipation by ions in the kev region, *Phys. Rev.* 124 (1961) 128–130. doi:[10.1103/PhysRev.124.128](https://doi.org/10.1103/PhysRev.124.128).
- [3] M. Norgett, M. Robinson, I. Torrens, A proposed method of calculating displacement dose rates, *Nuclear Engineering and Design* 33 (1) (1975) 50 – 54. doi:[http://dx.doi.org/10.1016/0029-5493\(75\)90035-7](http://dx.doi.org/10.1016/0029-5493(75)90035-7).
- [4] K. Nordlund, J. Wallenius, L. Malerba, Molecular dynamics simulations of threshold displacement energies in fe, *Nuclear Instruments and Methods in Physics Research Section B: Beam Interactions with Materials and Atoms* 246 (2) (2006) 322 – 332. doi:<http://dx.doi.org/10.1016/j.nimb.2006.01.003>.
- [5] N. Juslin, B. Wirth, Simulation of threshold displacement energies in fecr, *Nuclear Instruments and Methods in Physics Research Section B: Beam Interactions with Materials and Atoms* 255 (1) (2007) 75 – 77, computer Simulation of Radiation Effects in Solids Proceedings of the Eighth International Conference on Computer Simulation of Radiation Effects in Solids (COSIRES 2006) Computer Simulation of Radiation Effects in Solids. doi:<https://doi.org/10.1016/j.nimb.2006.11.046>.
- [6] J. F. Ziegler, J. P. Biersack, M. D. Ziegler, SRIM: the stopping and range of ions in matter, Cadence Design Systems, Raleigh, NC, 2008.
- [7] R. Stoller, 1.11 - primary radiation damage formation, in: R. J. Konings (Ed.), *Comprehensive Nuclear Materials*, Elsevier, Oxford, 2012, pp. 293 – 332. doi:<https://doi.org/10.1016/B978-0-08-056033-5.00027-6>.
- [8] K. Nordlund, S. J. Zinkle, A. E. Sand, F. Granberg, et al., Improving atomic displacement and replacement calculations with physically realistic damage models, *Nature Communications* 9 (2018) 1084.
- [9] O. B. Firsov, A qualitative interpretation of the mean electron excitation energy in atomic collisions, *JETP* 9 (5) (1959) 1076.
- [10] M. W. Finnis, P. Agnew, A. J. E. Foreman, Thermal excitation of electrons in energetic displacement cascades, *Phys. Rev. B* 44 (1991) 567–574. doi:[10.1103/PhysRevB.44.567](https://doi.org/10.1103/PhysRevB.44.567).
- [11] A. Caro, M. Victoria, Ion-electron interaction in molecular-dynamics cascades, *Phys. Rev. A* 40 (1989) 2287–2291. doi:[10.1103/PhysRevA.40.2287](https://doi.org/10.1103/PhysRevA.40.2287).
- [12] K. Nordlund, M. Ghaly, R. S. Averback, M. Caturla, T. Diaz de la Rubia, J. Tarus, Defect production in collision cascades in elemental semiconductors and fcc metals, *Phys. Rev. B* 57 (1998) 7556–7570. doi:[10.1103/PhysRevB.57.7556](https://doi.org/10.1103/PhysRevB.57.7556).

- [13] D. Duffy, A. Rutherford, Including the effects of electronic stopping and electron–ion interactions in radiation damage simulations, *Journal of Physics: Condensed Matter* 19 (1) (2006) 016207.
- [14] A. Rutherford, D. Duffy, The effect of electron–ion interactions on radiation damage simulations, *Journal of Physics: Condensed Matter* 19 (49) (2007) 496201.
- [15] J. le Page, D. R. Mason, W. M. C. Foulkes, The ehrenfest approximation for electrons coupled to a phonon system, *Journal of Physics: Condensed Matter* 20 (12) (2008) 125212. doi:10.1088/0953-8984/20/12/125212.
- [16] C. Race, D. Mason, A. Sutton, A new directional model for the electronic frictional forces in molecular dynamics simulations of radiation damage in metals, *Journal of Nuclear Materials* 425 (1) (2012) 33 – 40, *microstructure Properties of Irradiated Materials*. doi:<https://doi.org/10.1016/j.jnucmat.2011.10.054>.
- [17] M. Warriar, U. Bhardwaj, H. Hemani, R. Schneider, A. Mutzke, M. Valsakumar, Statistical study of defects caused by primary knock-on atoms in fcc cu and bcc w using molecular dynamics, *Journal of Nuclear Materials* 467 (2015) 457–464.
- [18] M. Warriar, U. Bhardwaj, S. Bukkuru, Multi-scale modeling of radiation damage: Large scale data analysis, in: *Journal of Physics: Conference Series*, No.1, Vol. 759, IOP Publishing, 2016, p. 012078.
- [19] U. Bhardwaj, S. Bukkuru, M. Warriar, Post-processing interstitialcy diffusion from molecular dynamics simulations, *Journal of Computational Physics* 305 (2016) 263 – 275. doi:<https://doi.org/10.1016/j.jcp.2015.10.034>.
- [20] S. Bukkuru, U. Bhardwaj, M. Warriar, A. Rao, M. Valsakumar, Identifying self-interstitials of bcc and fcc crystals in molecular dynamics, *Journal of Nuclear Materials* 484 (2017) 258–269.
- [21] M. Warriar, U. Bhardwaj, Molecular dynamics simulations of angular averaged displacement energy probabilities, Bhabha Atomic Research Centre Report BARC/2018/I/5.